PMSM drive with adaptive state feedback speed controller

R. SZCZEPANSKI[1]*, T. TARCZEWSKI[1], and L.M. GRZESIAK[2]

[1] Department of Automatics and Measurement Systems, Nicolaus Copernicus University, Grudziadzka 5, 87-100 Torun, Poland
[2] Institute of Control and Industrial Electronics, Warsaw University of Technology, Koszykowa 75, 00-662 Warsaw, Poland

Abstract. In this paper, the issue related to control of the plant with nonconstant parameters is addressed. In order to assure the unchanged response of the system, an adaptive state feedback speed controller for permanent magnet synchronous motor is proposed. The model-reference adaptive system is applied while the Widrow-Hoff rule is used as adjustment mechanism of controller's coefficients. Necessary modifications related to construction of the cost function and formulas responsible for adjustment of state feedback speed controller's coefficients are depicted. The impact of adaptation gain, which is the only parameter in proposed adjustment mechanism, on system behaviour is experimentally examined. The discussion about computational resources consumption of the proposed adaptation algorithm and implementation issues is included. The proposed approach is utilized in numerous experimental tests on modern SiC based drive with nonconstant moment of inertia. Comparison between adaptive and nonadaptive control schemes is also shown.

Key words: adaptive control, state feedback controller, PMSM, Widrow-Hoff rule.

1. Introduction

The efficiency, compact construction and reliability are important properties of electrical motors applied in many applications e.g. industrial robots, computerized numerical control (CNC) machines, ventilation and air conditioning systems, electrical and hybrid vehicles [1, 2]. For this reason, the permanent magnet synchronous motors (PMSMs) have received significant attention in researcher's community. The possibilities of the PMSM are not fully utilized by the commonly applied cascade of PID controllers, therefore a cascade-free controller structures are intensively investigated [3–7]. As it was shown in [5], the cascade-free state feedback controller (SFC) provides better dynamics and disturbance compensation in comparison to cascade control structure. Although tuning process of SFC is more complex in comparison to cascade control structure, it can be accomplished by using linear-quadratic optimization or pole placement technique. A relatively new approach is based on nature-inspired optimization algorithms where optimal coefficients of SFC are calculated automatically [8]. It should be emphasized that above mentioned methods select coefficients of SFC for nominal values of the plant parameters. It is well known that non-constant plant parameters may provide unsatisfactory behaviour of the system if controller with constant coefficients is used. In industry applications, deterioration of the system response can cause poor product quality or even production line failure. To prevent such occurrence, the coefficients of controller have to be adjusted to the actual operating point. As a result, independence of system response to the plant parameter changes is expected. Due to this, adaptive control seems to be necessary in modern high-performance electrical drive.

Adaptive controller is the structure that changes its behaviour in response to disturbance and plant uncertainty. The adaptation is based on adjustable coefficients and adjustment mechanism. The adaptive controller allows to improve functionality and performance. There are many adaptive schemes: model-reference adaptive system, gain scheduling, self-oscillating adaptive systems, self-tuning regulators, real-time estimation and robust high-gain control. Adaptive controllers are applied in many fields e.g. speed control of PMSM drive [9], control of induction motor drive [10], two-mass induction motor drive [11], tractor-trailer mobile robot [12], control of chaotic system [13], control of spacecrafts [14], magnetic microrobot controller [15], robotic ankle exoskeleton controller [16] and MEMS triaxial gyroscope controller [17]. Among all the model-reference adaptive system (MRAS) is one of the main adaptive control approaches [18–20]. MRAS has received significant attention in last years. The MRAS principle is to maintain constant response even if plant parameters have changed. This approach seems to be necessary in many industrial applications. In [21], application of MRAS for sensorless vector control of induction motor drive is shown. The sensorless control is responsive to induction motor parameters, i.e. stator and rotor resistances. In order to achieve proper speed estimation over parameters variation, the MRAS is utilized. In [22], adaptive SFC for two-mass system based on MRAS is shown. In this approach, a hybrid control structure is used: PI controller is responsible for current control while SFC is applied for speed control. The adaptive speed controller for PMSM drive based on nature-inspired

R. Szczepanski, T. Tarczewski and L.M. Grzesiak

optimization algorithm and the MRAS is proposed in [23]. The Artificial Bee Colony optimization algorithm is applied as adjustment mechanism. In order to assure proper operation of this adaptive controller, the periodic reference signal is necessary.

Since the goal of MRAS is to keep response of the plant the same as reference model regardless of parameter's changes, it requires the adjustment mechanism responsible for updating coefficients of controller. The basic approaches of the adjustment mechanism in MRAS are: the gradient approach, Lyapunov function and passivity theory. The Widrow-Hoff rule (W-H) is based on the idea of gradient approach and it was also recently applied as adjustment mechanism in MRAS with hybrid, cascade control structure [22]. Initially, the W-H rule was proposed in 1960 to train the adaptive pattern classification machine called Adaline, for adaptive linear neuron [24]. This method is also called Least Mean Square (LMS) method and it is a class of adaptive filters. Only the error at current time is used to adjust the weights. The form of learning principle depends on the model structure and it is based on the instantaneous gradient of the model output with respect to the weight vector.

In this paper, application of W-H as adjustment mechanism of MRAS is proposed, in order to obtain unchanged behaviour of the PMSM drive for the moment of inertia variations. The required balance between the time of convergence and the generalization of algorithm is discussed and proved by experiments. Implementation issues of the most important parts of the adaptive state feedback speed controller (ASFC) are included. Proposed adaptive control algorithm is examined in experimental tests. To the best authors' knowledge this is the first time when the MRAS with W-H is applied to full-state feedback speed controller for PMSM drive. The preliminary research results of this paper were presented at the 14th Conference "Sterowanie w Energoelektronice i Napędzie Elektrycznym SENE 2019" [25], while this paper is extended by (i) the additional experimental research and (ii) discussion about impact of adaptation gain on adaptation process. Designing of state feedback speed controller based on linear-quadratic optimization method has been described. Dynamic behavior of the proposed adaptive control scheme has been compared with non-adaptive one.

2. State feedback speed controller for PMSM drive

Designing process of adaptive state feedback controller is divided into two main stages. Firstly, state feedback speed controller is designed. Next, coefficients' adjustment method is introduced. Synthesis of state feedback speed controller requires knowledge of mathematical model of the plant (i.e. PMSM fed by VSI). Therefore linear model has been described in state space representation as follows [23]

$$\frac{d\mathbf{x}_i(t)}{dt} = \mathbf{A}_i\mathbf{x}_i(t) + \mathbf{B}_i\mathbf{u}_i(t) + \mathbf{F}_i r_i(t) \tag{1}$$

with

$$\mathbf{A}_i = \begin{bmatrix} -\dfrac{R_s}{L_s} & 0 & 0 & 0 \\ 0 & -\dfrac{R_s}{L_s} & 0 & 0 \\ 0 & \dfrac{K_t}{J_m} & -\dfrac{B_m}{J_m} & 0 \\ 0 & 0 & 1 & 0 \end{bmatrix}, \quad \mathbf{B}_i = \begin{bmatrix} \dfrac{K_p}{L_s} & 0 \\ 0 & \dfrac{K_p}{L_s} \\ 0 & 0 \\ 0 & 0 \end{bmatrix},$$

$$\mathbf{F}_i = \begin{bmatrix} 0 \\ 0 \\ 0 \\ -1 \end{bmatrix}, \quad \mathbf{x}_i(t) = \begin{bmatrix} i_d(t) \\ i_q(t) \\ \omega(t) \\ x_\omega(t) \end{bmatrix}, \quad \mathbf{u}_i(t) = \begin{bmatrix} u_{ld}(t) \\ u_{lq}(t) \end{bmatrix},$$

$$r_i(t) = \omega_{ref}(t)$$

where: R_s, L_s are resistance and inductance of the PMSM, J_m is moment of inertia, K_t is torque constant, B_m is viscous friction, $i_d(t)$, $i_q(t)$ are current space vector components, $\omega(t)$ is angular velocity of the PMSM shaft, K_p is gain of voltage source inverter, $u_{ld}(t)$, $u_{lq}(t)$ are linear components of control voltages, $\omega_{ref}(t)$ is reference value of angular velocity. In order to ensure steady-state error-free operation for step changes of reference velocity, the $x_\omega(t)$ state-space variable has been introduced and specified by the following formula [26]

$$x_\omega(t) = \int_0^t \left[\omega(\tau) - \omega_{ref}(\tau) \right] d\tau. \tag{2}$$

Depicted above state variable corresponds to the integrator and it is commonly used in order to assure the error-free steady-state operation. This approach is commonly applied to design a type 1 servo system when the plant has no integrator and the state feedback controller is utilized [26].

The control law for the SFC is defined as

$$\mathbf{u}_i(n) = \mathbf{K}\mathbf{x}_i(n) = \begin{bmatrix} k_{x1} & k_{x2} & k_{x3} & k_{\omega1} \\ k_{x4} & k_{x5} & k_{x6} & k_{\omega2} \end{bmatrix} \mathbf{x}_i(n) \tag{3}$$

where: n is a discrete sample time index, $k_{x1}-k_{x6}$ and $k_{\omega1}$, $k_{\omega2}$ are gain coefficients of SFC. The initial coefficients of SFC used in this work have been selected by trial and error method based on experience of the authors. The selected $\mathbf{Q}$ and $\mathbf{R}$ matrices are as follows

$$\mathbf{Q} = diag\left(\begin{bmatrix} 7.2 \cdot 10^{-3} & 7.2 \cdot 10^{-3} & 7.2 \cdot 10^{-3} & 4.0 \end{bmatrix} \right),$$

$$\mathbf{R} = diag\left(\begin{bmatrix} 1.0 & 1.0 \end{bmatrix} \right).$$

These matrices are used to linear-quadratic optimization that minimizes discrete performance index given by following formula:

$$I_{LQR} = \sum_{n=0}^{\infty} \left[\mathbf{x}_i^T(n)\mathbf{Q}\mathbf{x}_i(n) + \mathbf{u}_{li}^T(n)\mathbf{R}\mathbf{u}_{li}(n) \right]. \tag{4}$$

Coefficients of controller obtained by linear-quadratic optimization are

$$\mathbf{K} = \begin{bmatrix} 0.148088768 & 0 \\ 0 & 0.0724559799 \\ 0 & 0.0980584696 \\ 0 & 1.99180281 \end{bmatrix}^T.$$

Since the proposed control scheme will be implemented in a prototype drive, the implementation of state feedback speed controller in microcontroller has following form (3)

```
1  urd = (−1)*(K[0][0]*id
2              +K[0][1]*iq
3              +K[0][2]*vel
4              +K[0][3]*i_e_vel);
5
6  urq = (−1)*(K[1][0]*id
7              +K[1][1]*iq
8              +K[1][2]*vel
9              +K[1][3]*i_e_vel);
```

where: *id* and *iq* are space vector current components in *d-q* coordinate system, *vel* and *i_e_vel* are the angular velocity and the integral of error between actual angular velocity and reference signal, and **K** is gain matrix of SFC. It is worth to point out that integral was calculated by using backward rectangle rule given by following formula

$$\int_{x_1}^{x_2} f(x)\,dx \approx (x_2 - x_1) f(x_2) \tag{5}$$

which in this particular case can be written as

$$x_\omega(t) = \int_0^t \left[\omega(\tau) - \omega_{ref}(\tau)\right] d\tau \approx \sum_{i=0}^{t/T_s} \Delta x_\omega(i \cdot T_s) \tag{6}$$

with

$$\Delta x_\omega(t) = \int_{t-T_s}^t \left[\omega(\tau) - \omega_{ref}(\tau)\right] d\tau \approx T_s \left[\omega(t) - \omega_{ref}(t)\right]$$

where: T_s is a sampling period, $\Delta x_\omega(t)$ is numerical integration of error between actual velocity and reference value, which is based on Eq. (5). In order to calculate the $x_\omega(t)$ the above mentioned value of numerical integration must be added to $x_\omega(t - T_s)$. The overall formula is represented by a sum of numerical integration values (6).

3. Model-Reference Adaptive System

One of the main approaches used in adaptive control is Model-Reference Adaptive System, which was proposed by Whitaker in 1958. The basic principle is related to adjustment of controller's parameters in order to achieve desired response equals to a reference signal determined by model [18]. The principle

of MRAS is shown in Fig. 1. It is worth to point out that model specifies the performance of a system and coefficients of controller are adjusted on the basis of the error between the reference model (y_m) and the plant response (y). Basic approaches of the analysis and design of a MRAS are: (i) the gradient approach, which has been used by Whitaker in the original work, (ii) Lyapunov function and (iii) passivity theory. The Widrow-Hoff rule (W-H) (Least Mean Square algorithm) is used as another approach of the MRAS design, due to similarity in data processing of SFC and the Adaline model [22].
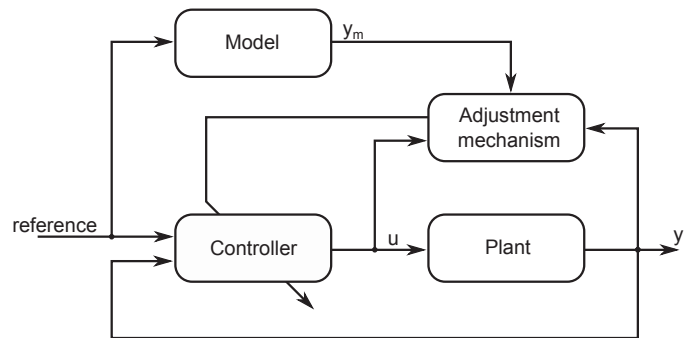

Fig. 1. Block diagram of a model-reference adaptive system

The implementation of MRAS to PMSM drive controlled by SFC is more complex than a book example of MRAS presented in Fig. 1, because it is multiple-input multiple-output (MIMO) control system. In order to adapt SFC, the correction formula for each coefficient is needed. Due to the use of surface permanent magnet synchronous motor and negligibly small difference between *d*-axis and *q*-axis inductance of PMSM stator, the reluctance torque does not occur and only the *q*-axis current generate electromagnetic torque. Therefore to maximize efficiency, the *d*-axis current should be zero. To provide unchanged behaviour of the PMSM drive system under moment of inertia variations, only the *q*-axis coefficients of SFC are adapting due to its responsibility for generating electromagnetic torque. For the same reason the coefficient k_{x4} (i.e. *d*-axis current gain for *q*-axis control signal) is constant. The block diagram of proposed control structure is shown in Fig. 2.

The Widrow-Hoff is based on the idea of gradient descent to search for the optimal condition. Similarly to Adaline weights, the modification of SFC coefficients can be defined as follows

$$k_{x5}(i+1) = k_{x5}(i) + \mu \frac{\partial E}{\partial k_{x5}},$$

$$k_{x6}(i+1) = k_{x6}(i) + \mu \frac{\partial E}{\partial k_{x6}}, \tag{7}$$

$$k_{\omega 2}(i+1) = k_{\omega 2}(i) + \mu \frac{\partial E}{\partial k_{\omega 2}}$$

where: μ is an adaptation gain and E is the function to optimize, which in Adaline model has the following formula

$$E\big(\mathbf{w}(i)\big) = \frac{1}{2}\left[d(i) - y(i)\right]^2 \tag{8}$$

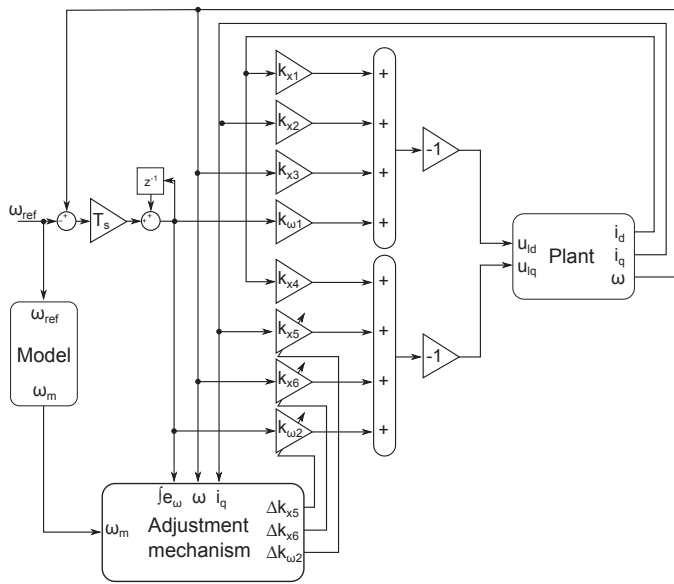R. Szczepanski, T. Tarczewski and L.M. Grzesiak

Fig. 2. Block diagram of proposed control scheme with SFC and MRAS

where: $d(i)$ and $y(i)$ are the desired and the actual output of the Adaline model. In order to apply W-H to SFC controller, the above mentioned formula (8) is modified to the following form

$$E\big(k_{x5}(i), k_{x6}(i), k_{\omega2}(i)\big) = \frac{1}{2}\big[e_{\omega\,MRAS}(i)\big]^2$$
$$= \frac{1}{2}\big[\omega_m(i) - \omega(i)\big]^2 \qquad (9)$$

where: $\omega_m(i)$ is response of model. The equations (7) and (9) derive the following formulas for the modification of SFC's coefficients

$$k_{x5}(i+1) = k_{x5}(i) - \mu e_{\omega\,MRAS}(i)i_q(i),$$
$$k_{x6}(i+1) = k_{x6}(i) - \mu e_{\omega\,MRAS}(i)\omega(i), \qquad (10)$$
$$k_{\omega2}(i+1) = k_{\omega2}(i) - \mu e_{\omega\,MRAS}(i)x_\omega(i).$$

These equations provide updated controller's coefficients in $(i+1)$-th discrete time index. One can see that coefficients are dependent on: (i) previous value of coefficient, (ii) difference between model response and plant velocity ($e_{\omega\,MRAS}(i)$), (iii) an adaptation gain (μ) and, (iv) state variable, that is associated with the corresponding controller's coefficient (i.e. i_q for k_{x5}, ω for k_{x6}, and $x_\omega(i)$ for $k_{\omega2}$).

4. Implementation issues

As it was previously depicted, MRAS approach is based on the required response of the model. In order to provide light and suitable shape of such a waveform for microcontroller implementation, the following methodology has been proposed: the model is based on simple digital low-pass filter given by fol-

lowing formula

$$x_f(i+1) = (1-\alpha)x_f(i) + \alpha x_m(i+1) \qquad (11)$$

where: x_f is filter output, α is low-pass filter coefficient, x_m is filter input, and mean of the M last reference signal values

$$x_m = \frac{1}{M}\sum_{i=0}^{M-1} x(i). \qquad (12)$$

Two-part methodology allows to obtain response of the second order model with low consumption of computation resources of microcontroller. It is possible to receive satisfying response of the MRAS using the following implementation

```
1  // Fast calculation of buffer sum
2  tmp = buffer[idx];
3  buffer[idx] = ref;
4
5  buffer_sum -= tmp;
6  buffer_sum += ref;
7
8  mean = buffer_sum / buffer_size;
9
10 // Simple low-pass filter
11 output = (1-lp_a) * output_prev + lp_a * mean;
12
13 if( ++idx >= buffer_size )
14     idx = 0;
15
16 output_prev = output;
```

The response of MRAS depends on two parameters: buffer size for mean calculations ($buffer\_size$) and low-pass filter coefficient (lp_a). The parameters have been manually selected to obtain required response of the drive and these are equal to 704 for buffer size and 0.00123 for low-pass filter coefficient. These correspond to the step response of the second order system with the rise time equal to 85 ms. The obtained shape of the MRAS compared to initially tuned SFC is shown in a further part of the article (the first column in Fig. 6).

The most obvious implementation of (10) is as follows

```
1  K[1][1] += (-1)*mi*e_mras*iq;
2  K[1][2] += (-1)*mi*e_mras*vel;
3  K[1][3] += (-1)*mi*e_mras*i_e_vel;
4
5  Calculation of urd and urq
```

where: mi is adaptation gain (μ), e_mras is the difference between actual angular velocity and the MRAS. The disadvantage of above implementation is related to partly loss of corrections, due to an accuracy of the 32-bit floating point numbers. For example, consider the following calculations with input value of parameters: $id = 0.1$, $iq = 1.5$, $vel = 5$, $i\_e\_vel = 0.2$, $vel\_ref = 10$, $e\_mras = 0.5$,
$K[0][0] = 0.148088768$,
$K[0][1] = K[0][2] = K[0][3] = K[1][0] = 0$,
$K[1][1] = 0.0724559799$,
$K[1][2] = 0.0980584696$,
$K[1][3] = 1.99180281$
and $mi = \mu = 2.5 \cdot 10^{-8}$. Comparison of the output signals for SFC and for ASFC is summarized in Table 1.

Table 1

Adaptation result of the most obvious implementation of ASFC with W-H rule (difference between SFC and ASFC values are blue)

Parameter	Value
urq (for SFC)	-0.997336864
updated $K[1][1]$	0.0724559575
updated $K[1][2]$	0.0980584100
updated $K[1][3]$	1.99180281
urq (for ASFC)	-0.997336864

It is worth to point out that values of necessary correction of coefficients for this example are $-1.87500007 \cdot 10^{-8}$, $-6.24999998 \cdot 10^{-8}$ and $-2.49999998 \cdot 10^{-9}$ for $K[1][1]$, $K[1][2]$ and $K[1][3]$, respectively. Values of correction are out of range of floating point accuracy, and necessary correction of coefficients is partly lost. Moreover, total correction of output signal (urq) is completely lost. In order to prevent such a phenomenon, the proposed implementation is based on two parallel SFCs: (i) with initial coefficients and (ii) with correction of initial coefficients. Depicted implementation is shown below

```
1  // Calculation of urd and urq for initial K
2
3  dK[1][1] += (-1)*mi*e_mras*iq;
4  dK[1][2] += (-1)*mi*e_mras*vel;
5  dK[1][3] += (-1)*mi*e_mras*i_e_vel;
6
7  urq_wh = (-1)*(dK[1][1]*iq
8               +dK[1][2]*vel
9               +dK[1][3]*i_e_vel);
10
```

```
11  urd += urd_wh;
12  urq += urq_wh;
```

For data used in a previous example, the output values of proposed implementation are summarized in Table 2. Thanks to the proper implementation, correction of the SFC's output has not been lost. Taking into account both implementations the proper one has better convergence due to increased accuracy of output signal corrections.

Table 2

Adaptation result of the proper implementation of ASFC with W-H rule (difference between SFC and ASFC values are blue)

Parameter	Value
urq (for SFC)	-0.997336864
$dK[1][1]$	$-1.87500007 \cdot 10^{-8}$
$dK[1][2]$	$-6.24999998 \cdot 10^{-8}$
$dK[1][3]$	$-2.49999998 \cdot 10^{-9}$
urq (for dK)	$3.41125002 \cdot 10^{-7}$
urq (for ASFC)	-0.997336507

In order to show the impact of adaptation algorithm to consumption of microcontroller computing resources, the execution time of each part of algorithm has been measured by internal timer of microcontroller. The execution time of ASFC implemented on STM32F407VGT6 running at 168 MHz has been shown in Fig. 3. It is worth to point out that the implementation of adaptation algorithm takes 2.048 μs, while the ASFC (i.e. generation of model-reference signal, adaptation algorithm, cal-
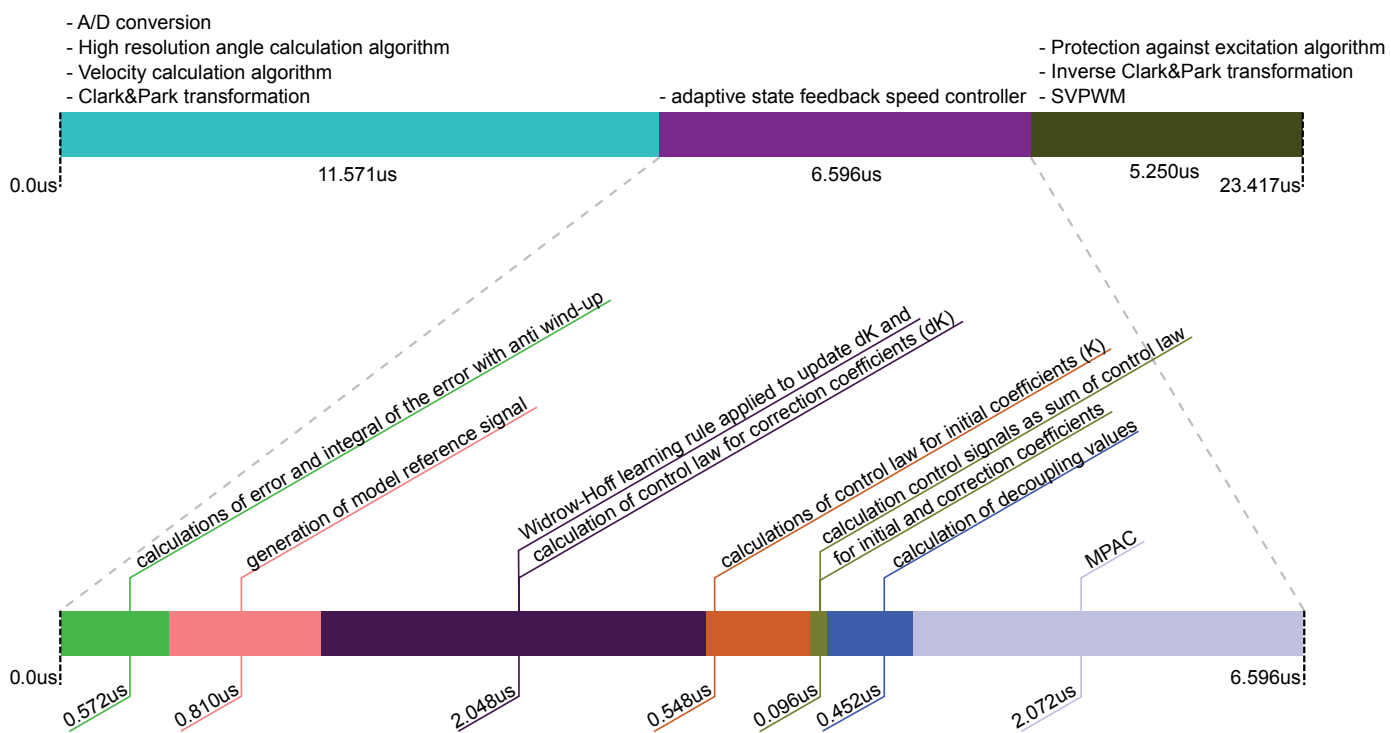

Fig. 3. Execution time of ASFC implemented in STM32F4@168MHz

culation of SFC output, taking into the account decoupling values, constraints handling method based on a posteriori model predictive approach (MPAC) [5]) takes 6.596 μs and the control loop with measurements, ASFC, Clark and Park transformations, space vector pulse width modulation (SVPWM) etc. takes 23.417 μs. The results of measured execution times can be used to determine the available switching frequency and it is up to 42.7 kHz.

5. Experimental results

Designed adaptive state feedback speed controller has been extensively investigated during experimental test. The laboratory stand used is equipped in 1.73 kW PMSM motor (LTi Drives LST-127-2-30-560) and two additional moment of inertias ($J_{nom} = 1.78 \cdot 10^{-2}$ kgm² and $J_{add} = 1.34 \cdot 10^{-2}$ kgm², respectively). The proposed ASFC has been implemented in STM32F407VGT6 microcontroller with ARM Cortex-M4 core and the sampling frequency was set to 22 kHz. Detailed description of the laboratory stand along with respective block diagram is available in [23], while the photo of its mechanical part is shown in Fig. 4.
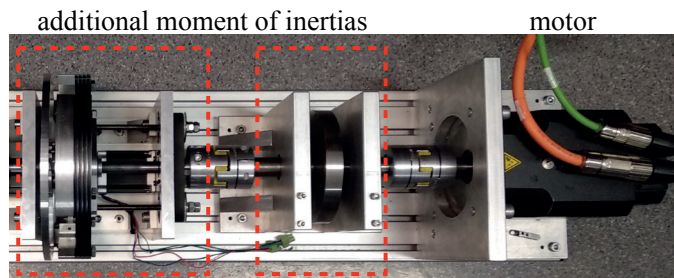
additional moment of inertias   motor

Fig. 4. The mechanical part of laboratory stand

The experimental examination of proposed ASFC has been divided into three tests:
- Test (I): initial fitness of manually selected coefficients during controller's synthesis to implemented MRAS,
- Test (II): moment of inertia increased to $J_{nom} + J_{add}$ (increased by 75.3%).

As it was mentioned earlier, the adaptation gain (μ) was manually selected by trial and error approach. It is worth to point out that higher value of μ allows to achieve faster convergence after disturbance or parameter variation. On the other hand, the higher value may also provide to over-fitting. In neural networks the term *over-fitting* describes situation, when error for training data set is very small, but for validation data set is large. This means that neural network fits to noises or corrupted data in training data set, which means the generalization of neural network is not proper. In adaptation process of ASFC, the over-fitting results in oscillating system response around the model-reference signal. It is worth to point out the allowed difference between the response of the system and the implemented MRAS was set to 0.2 rad/s. For smaller value of the difference, the value of e_mras is cleared. The allowed margin of error was set to avoid adaptation to unmodeled behaviour of the plant (e.g. cogging torque). Better generalization of adaptation process can be achieved by decreasing the adaptation gain. The adaptation gain was manually set to $\mu = 2.3 \cdot 10^{-7}$ by trial and error approach in order to receive good convergence, local minima avoidance and immunity to measurement noises. The impact of adaptation gain to system response for ASFC is shown in Fig. 5. The values of initial controller coefficients and moment of inertia variation responds to Test (II). It is worth to point out that higher value of adaptation gain provides a better convergence, but at 2.5 second one can see oscillations around model-reference, which finally leads to unstability of PMSM drive (the protection against excitation algorithm turned off the modulation signal to prevent damage of the
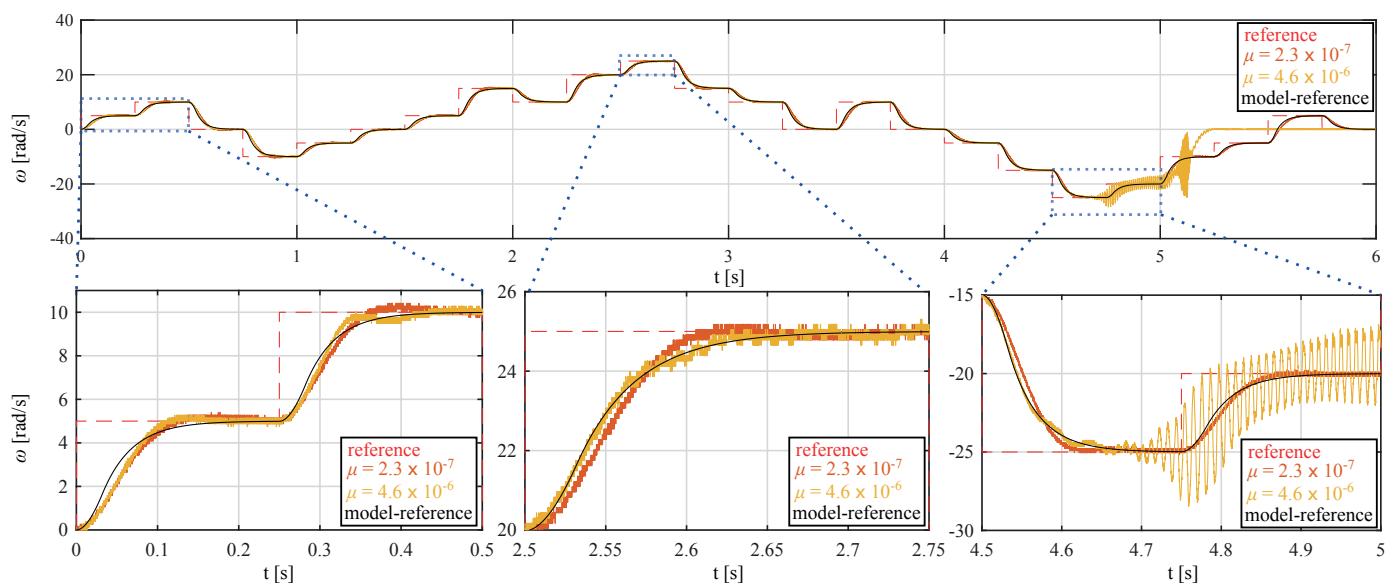

Fig. 5. Impact of adaptation gain (μ) on system response for ASFC

drive system). Stable operation of the drive for adaptation gain equals to $2.3 \cdot 10^{-7}$ can also be seen in the Fig. 9 at the second column. After 150 seconds of experiment, the coefficients stabilize and remain constant for next 100 seconds of experiment, which proves the immunity to measurement noises and good generalization.

The reference signal is a square wave with frequency equals to 1 Hz, amplitude 5 rad/s and offset 5 rad/s, which causes the steps to 10 rad/s and to 0 rad/s sequentially at every 0.5 s. Every test last for 250 cycles of reference signal. Due to significant number of cycles in every test, only the first and the last periods are presented in order to observe the impact of adaptation algorithm to plant's response. It should be noted that first period represents non-adaptive controller, i.e. constant coefficients (change of coefficients in first period is negligible small), while the last period presents the response after adaptation. The angular velocity and currents for the above mentioned periods are presented in Figs. 6, 7 and 8.
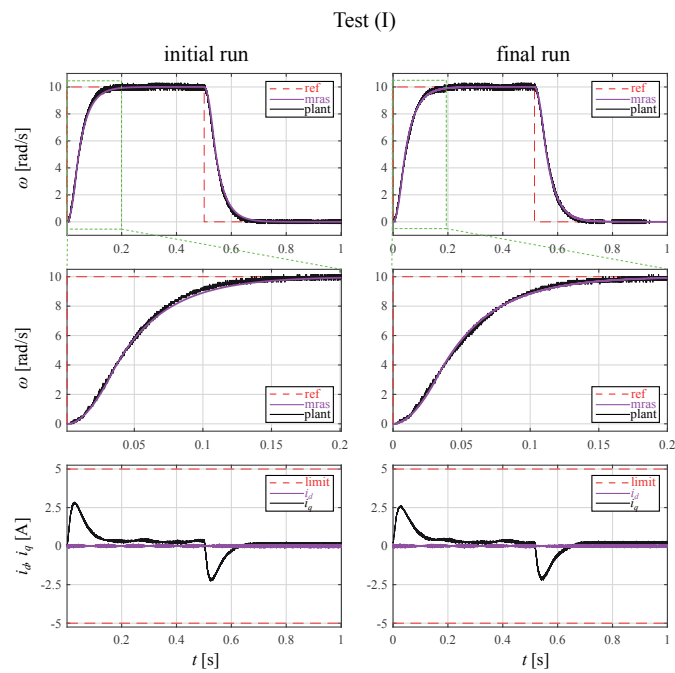

Fig. 6. Angular velocity and current for the first and the last period of reference signal obtained for test (I) (i.e. initial fitness to implemented MRAS)

In order to present the progress of the adaptation process, the fitness function is introduced

$$fitness(i) = \sum_{j=0}^{N} |\omega(i,j) - \omega_m(i,j)| \qquad (13)$$

where: i is reference signal period number, N is number of samples per reference signal period, j is sample time index within i-th reference signal period. The fitness function and coefficients of SFC obtained during adaptation for tests (I)–(III) are presented in Fig. 9.

From the obtained results, one can see that ASFC allows to receive similar response regardless of moment of inertia varia-
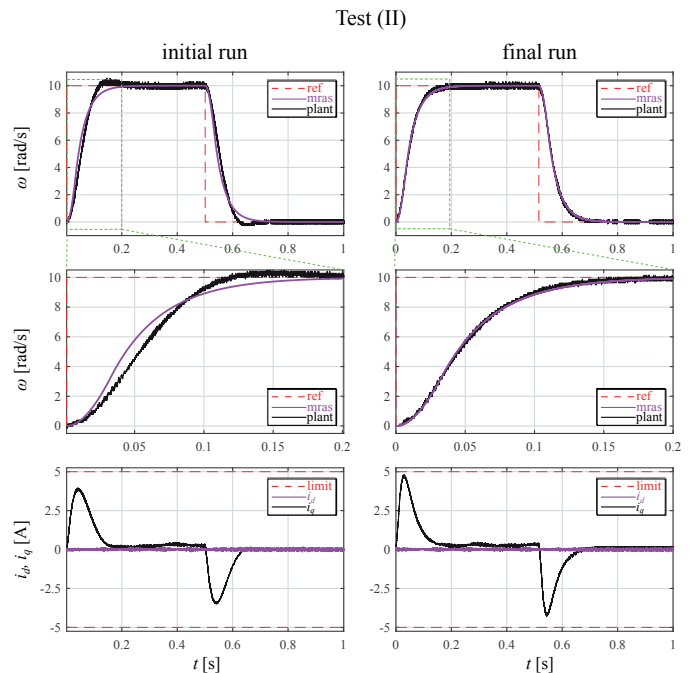

Fig. 7. Angular velocity and current for the first and the last period of reference signal obtained for test (II) (i.e. moment of inertia changed from J_{nom} to $J_{nom} + J_{add}$)
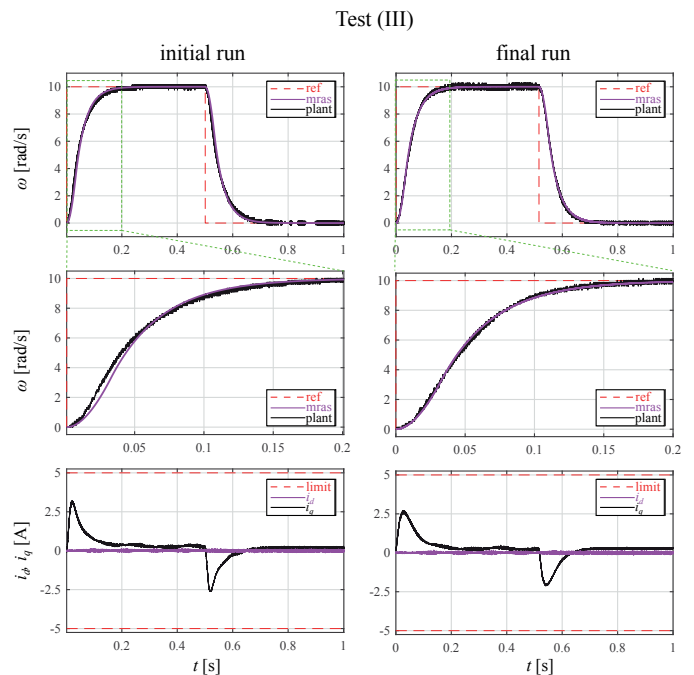

Fig. 8. Angular velocity and current for the first and the last period of reference signal obtained for test (III) (i.e. moment of inertia changed from $J_{nom} + J_{add}$ to J_{nom}

tion. The fitness function is noticeable decreased by the adaptation algorithm. Taking into account the first and the last period of reference signal, the fitness function has been decreased by 28.5%, 71.2% and 42.3% for test (I), (II) and (III), respectively. It is worth to point out that first period of reference signal is re-
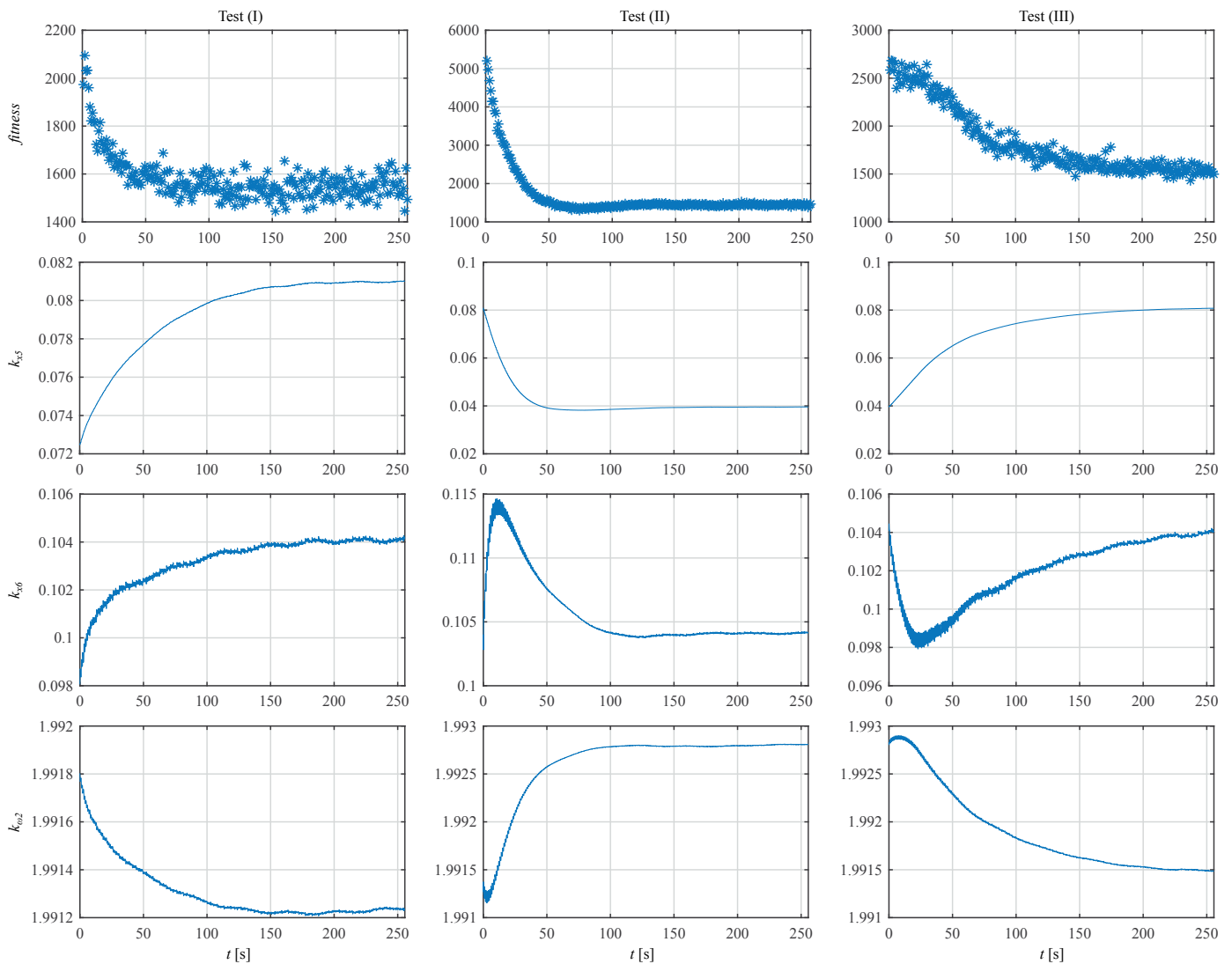
R. Szczepanski, T. Tarczewski and L.M. Grzesiak

Fig. 9. Fitness function and coefficients of the ASFC during adaptation for test (I)–(III)

sponse similar to non-adaptive controller, what means the above mentioned values may be interpreted as a profit of application the proposed adaptive approach in comparison to state feedback speed controller with constant coefficients.

The coefficients of SFC were stabilized within preselected number of reference signal cycles. It is worth to point out that chosen coefficient of adaptation gain (μ) provides good convergence and immunity to unmodeled measurement noises, cogging torque and other non-linearities of the control system.

6. Conclusions

The proposed ASFC is based on MRAS with W-H and it has been implemented in modern PMSM drive and examined for moment of inertia variations. The obtained results confirm that utilized methodology, designing and implementation of adaptive control system are valid. The W-H used to update coefficients of SFC ensures the same dynamics of PMSM regard-

less plant's parameter changes. Selection of adaptation gain for proposed ASFC has been well-founded by experimental tests. The adaptation time may be decreased by increasing the adaptation gain, but the over-fitting problem may occur, what is unacceptable in industrial applications. As it was presented in this paper, the application of proposed adaptive controller assures desired system response, in contrast to the non-adaptive controller, where response is prone to the inertia value.

Since the computation time of the main parts of adaptation algorithm (i.e. MRAS generation with calculation of corrections of SFC output signal) is equal to 2.954 μs, the time needed for the whole control loop is equal to 23.417 μs. Due to this it is worth to point out that the computation time needed for calculation of the MRAS has minor impact on the time required for execution of the whole control loop. Information important for practitioners and related to implementation issues is also shown. Finally, from depicted results one can see that it is possible to implement MRAS control scheme in drive with low-cost microcontroller and with high switching frequency.

REFERENCES

[1] S. Morimoto, "Trend of permanent magnet synchronous machines", *IEEJ Trans. Electr. Electron. Eng.* 2 (2), 101–108 (2007).

[2] C. Mi and M.A. Masrur, *Hybrid electric vehicles: principles and applications with practical perspectives*, John Wiley & Sons, 2017.

[3] T. Tarczewski, M. Skiwski, L.J. Niewiara, and L.M. Grzesiak, "High-performance PMSM servo-drive with constrained state feedback position controller", *Bull. Pol. Ac.: Tech.* 63 (1), 49–58 (2018).

[4] X. Liu, D. Wang, and Z. Peng, "Cascade-Free Fuzzy Finite-Control-Set Model Predictive Control for Nested Neutral Point-Clamped Converters With Low Switching Frequency", *IEEE Trans. Control Syst. Technol.* 27 (5), 2237–2244 (2019).

[5] T. Tarczewski and L.M. Grzesiak, "Constrained state feedback speed control of PMSM based on model predictive approach", *IEEE Trans. Ind. Electron.* 63 (6), 3867–3875 (2015).

[6] D. Horla and A. Krolikowski, "LQG/LTR control of input-delayed discrete-time systems", *Bull. Pol. Ac.: Tech.* 67 (6), 1049–1058 (2019).

[7] D. Dobrowolski, J. Dobrowolski, W. Piekarska, and S. Stępień, "Fast optimal feedback controller for electric linear actuator used in spreading systems of road spreaders", *Bull. Pol. Ac.: Tech.* 67 (6), 1041–1047 (2019).

[8] T. Tarczewski and L.M. Grzesiak, "An application of novel nature-inspired optimization algorithms to auto-tuning state feedback speed controller for PMSM", *IEEE Trans. Ind. Appl.* 54 (3), 2913–2925 (2018).

[9] T. Pajchrowski and K. Zawirski, "Application of artificial neural network for adaptive speed control of PMSM drive with variable parameters", *Compel-Int. J. Comp. Math. Electr. Electron. Eng.* 32 (4), 1287–1299 (2013).

[10] T. Orlowska-Kowalska and M. Dybkowski, "Performance analysis of the sensorless adaptive sliding-mode neuro-fuzzy control of the induction motor drive with MRAS-type speed estimator", *Bull. Pol. Ac.: Tech.* 60 (1), 61–70 (2012).

[11] T. Orlowska-Kowalska, M. Dybkowski, and K. Szabat, "Adaptive sliding-mode neuro-fuzzy control of the two-mass induction motor drive without mechanical sensors", *IEEE Trans. Ind. Electron.* 57 (2), 553–564 (2009).

[12] A.K. Khalaji and S.A.A. Moosavian, "Robust adaptive controller for a tractor–trailer mobile robot", *IEEE-ASME Trans. Mechatron.* 19 (3), 943–953 (2013).

[13] S. Vaidyanathan, "Adaptive controller and synchronizer design for the Qi-Chen chaotic system", in *Procedings of International Conference on Computer Science and Information Technology*, 124–133 (2012).

[14] F.K. Yeh, "Sliding-mode adaptive attitude controller design for spacecrafts with thrusters", *IET Contr. Theory Appl.* 4 (7), 1254–1264 (2010).

[15] L. Laurent, M. Fruchard, and A. Ferreira, "Adaptive controller and observer for a magnetic microrobot", *IEEE Trans. Robot.* 29 (4), 1060–1067 (2013).

[16] J. Koller, "Learning to walk with an adaptive gain proportional myoelectric controller for a robotic ankle exoskeleton", *J. NeuroEng. Rehabil.* 12 (1), 97 (2015).

[17] J. Fei and M. Xin, "An adaptive fuzzy sliding mode controller for MEMS triaxial gyroscope with angular velocity estimation", *Nonlinear Dyn.* 70 (1), 97–109 (2012).

[18] K.J. Åström and B. Wittenmark, *Adaptive control*, Courier Corporation, 2013.

[19] K.S. Narendra, *Applications of adaptive control*, Elsevier, 2012.

[20] N. Hovakimyan and C. Cao, *L1 Adaptive Control Theory: Guaranteed Robustness with Fast Adaptation*, Society for Industrial and Applied Mathematics, 2010.

[21] R. Kumar, "Review on model reference adaptive system for sensorless vector control of induction motor drives", *IET Electr. Power Appl.* 9 (7), 496–511 (2015).

[22] M. Kamiński, "Zastosowanie algorytmu BAT w optymalizacji obliczeń adaptacyjnego regulatora stanu układu dwumasowego", *Prz. Elektrotechniczny* 93 (1), 300–304 (2017) [in Polish].

[23] R. Szczepanski, T. Tarczewski, and L.M. Grzesiak, "Adaptive state feedback speed controller for PMSM based on Artificial Bee Colony algorithm", *Appl. Soft. Comput.* 83, 105644 (2019).

[24] B. Widrow and M.E. Hoff, "Adaptive switching circuits", Stanford Univ., CA, Stanford Electronics Labs, no. TR-1553-1 (1960).

[25] R. Szczepanski, T. Tarczewski, and L.M. Grzesiak, "PMSM drive with adaptive state feedback speed controller", in *Procedings of Conference Sterowanie w Energoelektronice i Napędzie Elektrycznym (SENE 2019)*, 2019.

[26] G.F. Franklin, J.D. Powell, and M.L. Workman, *Digital control of dynamic systems*, Addison-Wesley, 1998.